An algorithm for the calculation of the light distribution in photovoltaic greenhouses

Title

An algorithm for the calculation of the light distribution in photovoltaic greenhouses

Author names and affiliations:

Marco Cossu[a,*], Luigi Ledda[b], Giulia Urracci[c], Antonella Sirigu[c], Andrea Cossu[d], Lelia Murgia[e], Antonio Pazzona[e], Akira Yano[a].

[a] *Faculty of Life and Environmental Science, Shimane University, 1060 Nishikawatsu, Matsue, Shimane 690-8504, Japan*

[b] *Department of Agriculture, Division of Agronomy and Plant genetics, University of Sassari, Viale Italia 39, 07100 Sassari, Sardinia, Italy*

[c] *Agris Sardegna, Department of Plant Science, Viale Trieste 111, 09123 Cagliari, Sardinia, Italy*

[d] *Food Science and Technology Department, University of California - Davis, Davis, CA 95616 USA*

[e] *Department of Agriculture, Division of Agricultural Engineering, University of Sassari, Viale Italia 39, 07100 Sassari, Sardinia, Italy*

***Corresponding author:**

Marco Cossu, PhD

Faculty of Life and Environmental Science

Shimane University

1060 Nishikawatsu, Matsue, Shimane 690-8504, Japan

Tel./fax: +81 852 32 6543

E-mail: marcocossu@uniss.it, marcocossu@life.shimane-u.ac.jp

Keywords: renewable energy, solar radiation, crop, model, shading

Abstract

This study introduces a novel algorithm to estimate the cumulated global radiation inside photovoltaic (PV) greenhouses at the desired time interval. The direct and scatter radiation were calculated on several observations points (OPs) inside the PV greenhouse. The PV panels were assimilated to polygons that can overlap the sun path seen from a specific OP. The algorithm was tested in a greenhouse with 50% PV cover ratio on the roof. The results were showed as the percentage ratio of the cumulated yearly global radiation with and without PV array on the roof

(G_{GR}), and used to draw maps of the light distribution on different canopy heights (from 0.0 to 2.0 m). The maps displayed the variability of the light distribution and the most adversely affected zones inside the PV greenhouse. The yearly G_{GR} increased with the canopy height on the zones under the plastic cover (G_{GR} from 59% at 0.0 m to 73% at 2.0 m), and decreased under the PV cover (G_{GR} from 57% at 0.0 m to 40% at 2.0 m). Most zones close to the side walls and the gable walls were the least affected by shading on all canopy heights. The different light distribution on the canopy heights showed that the incident solar energy on the crop changes consistently, according to the growth stage of the plants. The algorithm can be applied to several PV greenhouse types and may provide a decision support tool for the identification of most suitable plant species, based on their light requirements.

1. INTRODUCTION

Renewable energy sources have increased the productivity and competitiveness of the agricultural sector, contributing positively to its environmental sustainability. The photovoltaic (PV) energy has been the most successful renewable source applied in European agriculture, primarily due to the long life, reliability and broad application of the technology. These features have been considered in the design of new crop systems, defined "agrivoltaic" systems, which integrate energy and food production on the same land unit (Dupraz et al., 2011). The PV greenhouse achieves this goal by integrating the PV panels on the roof. This is useful especially in locations where the land resource is limited (Dinesh and Pearce, 2016). These structures are particularly efficient in high solar irradiation regions, such as southern Europe (Campiotti et al., 2008). The high economic incentives provided by some European countries for PV energy generation in the last 7 years triggered the construction of new large PV greenhouse installations (Cossu et al., 2014; Fatnassi et al., 2015). Most european PV greenhouses attempted to maximize the profits deriving from the public subsidies and the electric energy sale by installing as much PV power as possible on the roof, without considering the light requirements of the crops. These issues address current researches to the agronomic sustainability of the PV greenhouse systems, focusing in particular on the design optimisation, the development of new PV technologies and the selection of plant species suitable for the solar light limitations inside PV greenhouses (Poncet et al., 2012).

The installation pattern of the PV panels on the roof affects the distribution of the solar radiation on the greenhouse area. Yano et al. showed that the checkerboard arrangement contributed to higher uniformity of light distribution in a gothic-arch roof greenhouse with 12.9% PV cover ratio, compared to the straight-line pattern (Yano et al., 2010; Fatnassi et al., 2015). The taller post height

of the greenhouse and the homogenous distribution of the PV power on the roof area allows more solar radiation to enter from the roof and the side walls (Cossu et al., 2010). The orientation and the shape of a greenhouse should aim to maximize the total energy input on the greenhouse area: the orientation with one face to West (W) and the other to East (E) results in the highest amount of energy captured in winter (El-Maghlany et al., 2015). For elliptical shape greenhouses, the best results are achieved by using high aspect ratios (ratio between height and width) to maximize the solar radiation incident per square meter of cultivated land.

Some PV technologies have been developed specifically for the application on greenhouse roofs, improving the light transmissivity of the whole system, respect to conventional panels. The promising PV technologies already studied on PV greenhouse systems were the CIG and CIGS semiconductors, the flexible PV and thin films, the organic PV cells and the semi-transparent PV panels, also based on spherical micro-cells (Cossu et al., 2016; Emmott et al., 2015; Marucci et al., 2012; Minuto et al., 2011; Yano et al., 2014). Other solutions include the use of Fresnel lenses, which can be integrated in the south (S) oriented roof to concentrate the sunlight and produce both electrical and thermal energy (Sonneveld et al., 2010; Chemisana et al., 2012). The possibility to adjust the shading level caused by the PV panels has been studied in a prototype dynamic PV greenhouse for Mediterranean areas, where the PV panels can rotate along the longitudinal axis (Marucci and Cappuccini, 2016a). The PV panels acted as a passive cooling system able to protect the crops from high internal temperature in summer, conciliating the energy production with the light requirements of the crops (Marucci and Cappuccini, 2016b). Indeed, by adjusting the shading level, more light can reach the crop, compared to a PV greenhouse with fixed panels.

The characterisation of the environmental conditions is essential to evaluate the agronomic sustainability of the PV greenhouses. In particular, the analysis should be conducted primarily on the available solar light and its distribution on the greenhouse area. Various studies have been conducted to provide decisional support for new design criteria and management of PV greenhouses. Some authors applied numerical simulations, including the Computational Fluid Dynamic (CFD) to assess the PV greenhouse microclimate in terms of solar radiation, temperature and air flow for specific summer and winter days (Fatnassi et al., 2015; Serrano-Arellano et al., 2015). The evolution of temperature and humidity inside PV greenhouses have been simulated also using the TRNSYS (Transient System Simulation Tool) software, highlighting that the winter night temperature inside a PV greenhouse underent a sudden fall until ambient temperature, while the summer temperature was too high for greenhouse crops (Carlini et al., 2010; Carlini et al., 2012). TRNSYS has been applied also to evaluate the solar water heating systems for greenhouse microclimate control, to calculate the productivity of the PV array, and to analyse the environmental parameters inside a prototype greenhouse equipped with semi-transparent PV panels and vertical

farm systems for urban agriculture (Attar and Farhat, 2015; Bambara and Athienitis, 2015). Geostastistics approaches have been used to assess the variability of the thermal spatial distribution, suggesting that the results of the crop growth models cannot be generalized for the entire greenhouse area due to the variability of the microclimate patterns (Bocaja et al., 2009). Yano et al. proposed an equation-based procedure to calculate the solar radiation impinging on a specific point located inside a PV greenhouse with 12.9% cover ratio, comparing the straight-line and a checkerboard installation pattern of the PV panels the roof (Yano et al., 2009; Yano et al., 2010). Castellano calculated the solar radiation distribution inside a greenhouse with different PV installation patterns and roof cover ratio on specific days, by using the software Autodesk® Ecotect® Analysis (Castellano, 2014; Castellano et al., 2016). The variability of the shade distribution was calculated as percentage of shading, which changed accordingly to the sun position, the configurations of the PV panels on the roof and the zones considered inside the greenhouse.

The software packages and the methods proposed in the literature calculate the light distribution only on a specific date and time, while the agronomic performance of the PV greenhouse should consider the cumulated light distribution on the crop cycle basis for a reliable yield estimation. In this paper, we propose a novel algorithm elaborated with the software Wolfram Mathematica, which can calculate the cumulated distribution of the solar radiation inside a PV greenhouse at the desired time interval, as a function of the shading cast by the PV array on the roof. The procedure is based on a geometric condition assimilating the PV panels to polygons that can overlap the sun path observed from specific observation points located inside the greenhouse. The calculation can be reiterated for multiple points and used to draw maps of cumulated light distribution on yearly basis and on different canopy heights. The validation was conducted on a real PV greenhouse with 50% cover ratio. This algorithm can be applied to various PV greenhouse types with different location, orientation, roof slope, PV cover ratio and installation patterns of the PV panels on the roof.

2. MATERIALS AND METHODS

2.1 Characteristics of the photovoltaic greenhouse

The algorithm was applied and validated on a commercial pitched-roof PV greenhouse in Decimomannu (Sardinia, Italy; 39°19'59"N, 8°59'19"E), already used by the authors for previous experiments concerning the measurement of the light distribution inside PV greenhouses (Cossu et al., 2014). The area of the greenhouse was 960 m^2 and it was provided with two spans (50.0 m long and 9.6 m wide each), gutter height of 2.5 m, roof slope of 22° and E−W orientation (Fig. 1). The plastic cover and the walls were made with PVC (Ondex Bio, Renolit, France). The cladding

materials and the PV panels were supported by a steel structure. The S oriented roof of each span was formed by 144 multi-crystalline silicon PV modules (REC 235PE, REC Solar, USA), with dimensions 1665×99×138 mm. As a result, 50% of the roof area was covered with PV modules. The total PV area was 475 m^2 (238 m^2 per span), while the total active cell area was 420 m^2. The peak rated power of the PV system was 68 kWp.

The cumulated yearly light distribution was calculated on different canopy heights (0.0, 0.5, 1.0, 1.5 and 2.0 m from the ground level). Calculations were conducted on 5 sets of observation points (OPs), each one formed by 27 OPs. Set G1 and G2 were located 1.5 m from the gable walls of the greenhouse. Set S1, S2 and S3 were placed equidistant. This distribution was chosen according to previous observations inside the same PV greenhouse, stating that the variability of the light distribution on the E-W direction is not statistically significant inside E-W oriented PV greenhouses (Cossu et al., 2014). For this reason, a lower amount of OPs is enough to quantify the distribution on the E-W direction (5 OPs), compared to the number of OPs on the N-S direction (27 OPs). In addition, the solar radiation incident on the zones close to the gable walls is different from what observed on the remaining area (Castellano, 2014). As a consequence, the evaluation of the incident light close to the gable walls is necessary to accurately describe the distribution on the whole PV greenhouse.

2.2 Algorithm for the calculation of the light distribution inside the photovoltaic greenhouse

2.2.1 Calculation of the incident global radiation

The position of the sun was determined using the solar elevation angle and the solar azimuth angle in radians for the whole year, at 1 hour interval (Fig. 2). The solar elevation angle (θ) has positive values above the horizon (0 rad on the horizon plane) and it was calculated according to the following equation (Markvart, 2000; Page, 2003; Yano et al., 2009):

$$\theta = Arcsin\,(Sin\phi\,Sin\delta + Cos\phi Cos\delta Cos\omega) \quad \text{(rad)} \quad (1)$$

where ϕ is the latitude of the site in radians, ω the hour angle and δ the solar declination angle (Markvart, 2000; Page, 2003):

$$\omega = \frac{\pi}{12}(LAT - 12) \quad \text{(rad)} \quad (2)$$

$$\delta = \pi \frac{23.45}{180} Sin\left(2\pi\ \frac{284+n}{365}\right) \quad \text{(rad)} \quad (3)$$

LAT is the local apparent time in hours and *n* is the number of the day in the year. *LAT* was calculated using the formula (Page, 2003):

$$LAT = LMT + \frac{(\lambda - \lambda_R)}{15} + E - c \quad \text{(h)} \quad (4)$$

where *LMT* is the local mean time of the site, also known as "clock time". λ is the longitude of the site and λ_R the longitude of the time zone of the site. The coefficient *c* is the correction of the equation during the summer time. *E* is the equation of time, expressed by the following formula (Markvart, 2000):

$$E = 2.292(0.0075 + 0.1868Cos\beta - 3.2077Sin\beta - 1.4615Cos2\beta - 4.089Sin2\beta) \quad \text{(rad)} \quad (5)$$

where β is an angle equal to:

$$\beta = \frac{2\pi(n-1)}{365} \quad \text{(rad)} \quad (6)$$

The azimuth angle Ψ of the sun is (Markvart, 2000; Page 2003):

$$\Psi = Arccos\left(\frac{sin\theta\ sin\phi - sin\delta}{cos\theta\ cos\phi}\right) \quad \text{(rad)} \quad (7)$$

This angle is 0 to the S direction and it is multiplied by -1 when $\sin\Psi<0$.

2.2.2 Calculation of the internal global radiation

The direct (I_d) and scatter (I_s) radiation on the horizontal plane were calculated according to the following formulas and assuming clear sky conditions (Berlage, 1928; Reiter et al., 1982; Palva et al., 2001; Tanaka et al., 2002; Kosugi et al., 2006):

$$I_d = I_0 \cdot p^{\frac{1}{Sin\theta}} \cdot Sin\theta \quad \text{(W m}^{-2}\text{)} \quad (8)$$

where I_0 is the solar constant (1367 W m^{-2}) and *p* the atmospheric transmissivity coefficient. The scatter radiation is:

$$I_s = \frac{I_0 Sin\theta (1 - p^{\frac{1}{Sin\theta}})}{2(1 - 1.4 Log\, p)} \quad (\text{W m}^{-2}) \tag{9}$$

The greenhouse global radiation on the horizontal plane I_G *(W m^{-2}),* considered as the sum of the direct and scatter radiation, can be expressed as:

$$I_G = \tau (I_d + I_s) \quad (\text{W m}^{-2}) \tag{10}$$

where τ is the overall light transmissivity of the greenhouse (frame and cover material). I_G can be considered as the incident global radiation inside the greenhouse without any PV panels installed on the roof. Therefore, this parameter was considered to calculate the global radiation inside the PV greenhouse as a function of the global radiation inside a conventional greenhouse.

2.2.3. Determination of the global radiation on a random OP inside the PV greenhouse

The functions used in the present algorithm were implemented in the software Wolfram Mathematica (Wolfram, 2014). To determine the actual solar radiation on the OPs, each PV panel on the greenhouse roof was considered as a polygon with 4 edges by using the geometric function "Polygon" of the software. The Cartesian coordinates (*x*,*y*,*z*) of the 4 edges and the OP were calculated as a function of an arbitrary point of origin located in the North (N)-E edge of the greenhouse. The Cartesian coordinates were converted into solar coordinates, thus elevation angle (θ_e) and azimuth angle (Ψ_e), in relation to a specific OP, by using the following expressions:

$$\theta_e = Arcsin \frac{z_e - z_{op}}{\sqrt{(x_e - x_{op})^2 + (y_e - y_{op})^2 + (z_e - z_{op})^2}} \quad \text{(rad)} \tag{11}$$

$$\Psi_e = Arccos \frac{y_e - y_{op}}{\sqrt{(x_e - x_{op})^2 + (y_e - y_{op})^2}} \quad \text{(rad)} \tag{12}$$

where x_e, y_e and z_e are the Cartesian coordinates of an edge of the PV panel, while x_{op}, y_{op} and z_{op} are the Cartesian coordinates of the OP considered. Ψ_e is equal to 0 on S and it was considered negative when $x_e - x_{op} < 0$, thus when it moved towards W.

The solar coordinates of the 4 edges of the PV panel ($\theta_e^{1,2,3,4}$, $\Psi_e^{1,2,3,4}$) were compared to the solar coordinates of the sun (θ, Ψ) seen from the OP, by using the function "Region Member" of the software, to verify when the solar coordinates cast on the PV panel surface area (Fig. 3). When the solar coordinates of the sun were inside the area of the polygon, the OP was considered under the shadow of the PV panel, thus without incident direct radiation. As a consequence, the global

radiation on the OP (I_{GP}) is equal to the scatter radiation ($I_{GP} = I_s$). On the contrary, when the sun coordinates were outside the area of the PV panel, the OP was considered under sunlight, thus receiving both direct and scatter radiation ($I_{GP} = I_d + I_s$). This procedure was applied simultaneously for all the panels of the PV system on a single OP and then reiterated for all OPs.

The incident global radiation on the PV greenhouse area (G_{GR}) was calculated as the mean percentage ratio of I_{GP} for all n OPs and the potential global radiation inside the same greenhouse without PV array on the roof (I_G):

$$G_{GR} = \frac{1}{n}\sum_{OP=1}^{n}\frac{I_{GP}}{I_G}\cdot 100 \quad (\%) \tag{13}$$

where n was varied to calculate the G_{GR} for specific zones of the PV greenhouse. Both I_{GP} and I_G were calculated considering the overall greenhouse transmissivity τ. As a consequence, G_{GR} is independent from τ and it describes the light distribution as a function of the PV greenhouse typology (dimensional parameters of the greenhouse and PV cover ratio), thus it assumes a general validity also when the same PV greenhouse is assembled in different locations and with different cladding materials.

2.2.4 Validation of the model

The model was validated by measuring the global radiation inside the real PV greenhouse on 12 days with clear sky (one per month), from May 2013 to April 2014. The measurements were conducted using 10 pyranometers (HOBO Silicon Pyranometer Sensor w/ 3m Cable - cod. S-LIB-M003; Onset Computer Corporation, Bourne, USA) placed at 1.3 m height, according to the pattern depicted in Figure 1. All data were collected with a single datalogger (HOBO Micro Station Logger G21-002; Onset Computer Corporation, Bourne, USA) at 1 min interval and averaged every 15 min. The external global radiation data were collected from the closest weather station located in Uta (Sardinia, Italy; 39°17'35.1"N 8°55'55.0"E). The sky transmissivity coefficient on the single day was estimated adjusting the calculated external global radiation to best correlate with the corresponding external measured values.

The mean greenhouse transmissivity was calculated on each sensor position from 7:00 to 18:00 h, as the ratio of the global radiation measured by the sensor and the external global radiation. To mitigate the effect of the shadow cast by the metallic frame on the roof (not considered by the present algorithm), the measurements of the sensors were corrected using the mean hourly greenhouse transmissivity: when the measured transmissivity on the sensor was lower than the daily mean greenhouse transmissivity, the values were adjusted by multiplying the daily mean transmissivity for the external global radiation. The validation was conducted using the Coefficient

of Determination (R^2) between measured and calculated data. The variability of the light distribution was studied using the Coefficient of Variation (CV), thus the ratio of the standard deviation and the mean global radiation on the OPs.

3. RESULTS AND DISCUSSION

3.1. Solar light distribution in the photovoltaic greenhouse

Depending on how the solar coordinates intersect the PV array coordinates, the OPs can be under three basic conditions: direct light, partial shading or complete shading (Fig. 4). The calculated data were compared to the 12 days measurements used for the validation, showing a mean R^2 of 0.87±0.10. In summer the solar elevation angle on OP F was high and the sun path moved above the PV array, leaving the OP under direct radiation for all day (June 16th 2013). Starting from the solstice in June, the elevation angle decreased till the sun path intersected the PV array, causing a partial shading (September 14th 2013). Finally, during winter the sun path was almost completely covered by the PV array and only the scatter light was received, determining a complete shading (December 14th 2013). On partial shading, the shadow usually cast on the OP during the central part of the day. However, depending on the period of the year and the greenhouse zone, the shadow can affect most part of the day, thus with direct radiation only in the morning or in the evening. The pyranometers showed fluctuations due to the intermittent shadow cast by the metallic frame of the roof, which occasionally shaded the direct radiation. For this reason, fluctuations were particularly accentuated when no shadow was on the OP (June 16th 2013), while they were mild or absent during partial or complete shading, since the scatter radiation was less affected by the metallic frame. However, the actual shadow cast by the frame was not considered in the present algorithm, which purpose is to estimate the light distribution inside PV greenhouses only as a function of the PV array, independently from the greenhouse frames types. This assumption allows the application of the present algorithm to a broad variety of PV greenhouse types.

According to the E-W orientation of the PV greenhouse, the shadow of the PV array moved from N to S in the first semester of the year, and from S to N in the second semester (Fig. 5). The E-W orientation enhances the global radiation incident in winter and decrease it in summer, when less irradiation is required by the crops (Sethi, 2009). During winter and most part of autumn, the sun elevation angle was low and the shadow cast mainly under the plastic cover, leaving the zones under the PV cover with direct radiation (Fig. 5a and 5d). As the sun elevation angle increased in springtime, the shadow gradually shifted under the PV array (Fig. 5b and 5c). This latter trend represents also the mean N-S distribution of the solar radiation during the year. In general, the less

affected zones were the ones under the plastic cover, especially from April to September, where the G_{GR} was nearly 100%.

The yearly cumulated light distribution maps inside the PV greenhouse are shown in Figure 6. The maps are presented at ground level (0.0 m) and at two canopy heights, for short crops (0.5 m) and tall crops (1.5 m). The N oriented span is occasionally affected by the shadow of the PV cover of the S oriented span. For this reason, the N span showed a G_{GR} averagely 6% lower than the S span during the year. This difference decreased as the canopy height increased and it was higher in winter (11% at 0.0 m) and not relevant in summer. The most shaded OPs under the PV cover received less than 31% G_{GR} on yearly basis, with the minimum value of 17% observed ad 1.5 m. The mean G_{GR} under the PV cover ranged from 40% (at 2.0 m) to 57% (at 0.0 m), while it ranged from 59% (at 0.0 m) to 73% (at 2.0 m) under the plastic cover. Some zones close to the side walls and the gable walls were the least affected by shading, with a yearly G_{GR} values over 91%, especially at 1.5 m.

The yearly mean G_{GR} on the PV greenhouse area was 56%, ranging from 57 at ground level to 55% at 1.5 m (Tab. 1). The G_{GR} under the plastic cover reached up to 100% in summer, indicating limited or no shading at 1.5 and 2.0 m height. The yearly G_{GR} under the plastic cover increased with the canopy height by 14% from 0.0 to 2.0 m, while it decreased by 17% under the PV cover (G_{GR} from 57 at 0.0 m to 40% at 2.0 m). In fact, an opposite trend can be observed under the PV cover, where the highest values of G_{GR} were found during winter at ground level (up to 77% in January and February), which were consistently higher than the ones under the plastic cover. The G_{GR} under the PV cover usually decreased in summer.

The yearly CV on the greenhouse area was averagely 56% on all canopy heights, showing that the distribution of the global radiation on the greenhouse area was characterised by a high spatial variability. The CV on the transversal direction (N-S) was 55% on average, due to the path of the shadow cast by the PV array and it was 35% on the longitudinal direction (E-W). However, the CV on the longitudinal direction of the central portion of the PV greenhouse (set S1, S2 and S3) was only 3%, independently from the canopy height. This was due to the path of the shadow, which moved mainly in the N-S direction, while it moved also in the E-W direction on the zones close the gable walls (set G1 and G2), adding variability to the longitudinal distribution of the whole PV greenhouse area. These results indicate that inside an E-W oriented PV greenhouse, the global radiation is heterogeneously distributed only in the N-S direction, but it can be considered uniform in the longitudinal direction for most of the greenhouse area, except the zones close to the gable walls.

3.2. Implications of the cumulated light distribution on the agronomic sustainability of photovoltaic greenhouses

The light distribution maps highlighted the effects of the shading on the greenhouse area. The cumulated distribution data provided with the present model at yearly and monthly basis can be considered important inputs for the crop management inside PV greenhouses. The dynamic movement of the shadow on the PV greenhouse area suggested that the scenarios of light distribution change consistently, according to the period of the year and the height of the canopy. In particular, the global radiation increased with the canopy height under the plastic cover, and it decreases under the PV cover. Therefore, the growth stage of the crop and the related canopy height should be carefully considered when running crop models for the yield estimation inside PV greenhouses. Only the zones under the plastic cover and close to the side walls are compatible with the profitable cultivation of greenhouse crops, given the direct relation between illumination and photosynthetic rate (Challa, 1989). Ornamental species or nursery could be raised on the side walls, also using optimized upper stacks, to exploit the higher solar radiation at taller heights under the plastic cover. This possibility was already successfully tested on nursery plants inside a E-W oriented greenhouse, where upper and lower stacks were placed on the N oriented side wall, without affecting the crop yield at ground level (Sethi and Dubey, 2011).

The negative effects of the shading on crop yield was already described on tomato, indicating the importance of maximizing the light transmission of the greenhouse (Cockshull et al., 1992). The PV cover ratio under 20% has been tested on basil, tomato and cucumber, resulting in no yield losses but negative effects on quality parameters, such as the fruit size and color (Ureña-Sánchez et al., 2012; Minuto et al., 2009). Therefore, this latter PV cover ratio should be considered the highest compatible with the most common greenhouse crops. Conversely, the cultivation of welsh onion suffered 25% yield loss inside a greenhouse with a PV cover ratio of 13% (Kadowaki et al., 2012). Furthermore, the insufficient solar radiation may cause a potential higher incidence of plant pathologies and require a specific crop protection approach. The cultivation cycle should start in a period with low shading, since heavy shading during juvenile stages may delay the development of the crop for the whole cycle (Marrou et al., 2013). As a consequence, for a PV greenhouse with 50% cover ratio, the cultivation should be conducted under the plastic cover and the cycle should start at the end of winter, to receive low or no shading during spring and summer.

Many greenhouses with high PV shading have been already constructed in Europe and their agronomic sustainability is still under discussion and scientific investigation. However, the design modification of existing PV greenhouses to achieve a higher irradiance is often not feasible under a technical and economic point of view, due to the high costs related to the partial reconstruction, including the modification of the PV panel installation patterns on the roof. For this reason, the

strategies to improve the agronomic productivity of preexisting PV greenhouses should necessarily consider the crop management and the identification of suitable crops with low light requirements. The light distribution maps can be considered a valid decisional support tool to identify the best species and the portions of the greenhouse area suitable for a successful cultivation. With the present algorithm, these maps can be calculated for the most diffused PV greenhouse types. Subsequently, crop models can use the information concerning the light distribution to estimate the yield and development, focusing also on specific crop protection strategies.

4. CONCLUSIONS

The agronomic sustainability of the PV greenhouse is strictly connected to the available incident global radiation and its distribution on the greenhouse area. The algorithm proposed in this paper is able to calculate the cumulated direct and scatter radiation on the PV greenhouse area at the desired time interval and on different canopy heights. Geometric functions assimilating the PV panels to polygons are used to calculate the shading cast by the PV panels on designated points inside the greenhouse. To characterize the light distribution only as a function of the PV greenhouse type, the results have been expressed as the ratio of the cumulated global radiation inside the greenhouse with and without PV array on the roof. The simulations were conducted on a real E-W oriented greenhouse with a 50% PV cover ratio. Remarkable differences were observed on the ratio between the internal global radiation and the potential greenhouse global radiation without PV panels. These values ranged from 59 to 73% under the plastic cover and from 40 to 57% under the PV cover, depending on the canopy height considered (from 0.0 to 2.0 m). The differences were shown through maps of cumulated light distribution, which highlighted the greenhouse zones receiving the highest amount of solar radiation, thus the most suitable for cultivation. This algorithm can be used in perspective as a decisional support tool for choosing and managing crops inside PV greenhouses, based on their light requirements. Further studies will focus on the calculation of the light distribution maps for various existing PV greenhouse types. The structures will be compared and studied according to the light requirements of common and not conventional greenhouse crops, attempting to identify the most sustainable types and the best practices for crop management inside the PV greenhouses.

ACKNOWLEDGEMENTS

The authors thank the Autonomous Region of Sardinia (Italy) for the financial support on the fundamental research project, LR 7/2007, "ORTILUX: Energy from photovoltaic greenhouse: study of the environmental parameters limiting the cultivation of tomato". We would like to thank also the Sardaflora-Cidam company and Mr. Murtas for his collaboration. This study was supported by Japan Society for the Promotion of Science (JSPS post-doctoral fellowship, Grant No. 26•04085).

REFERENCES

1. Attar, I., Farhat, A., 2015. Efficiency evaluation of a solar water heating system applied to the greenhouse microclimate. Sol. Energy 119:212–224. http://dx.doi.org/10.1016/j.solener.2015.06.040.
2. Bambara, J., Athienitis, A., 2015. Experimental evaluation and energy modeling of a greenhouse concept with semi-transparent photovoltaics. Energy Procedia 78, 435–440. doi:10.1016/j.egypro.2015.11.689.
3. Berlage, H.P., 1928. Zur Theorie der Beleuchtung einer horizontalen Fläche durch Tageslicht. Meteorologische Zeitschrift, 45(5): 174–180.
4. Bojacá, C.R., Gil, R., Cooman, A., 2009. Use of geostatistical and crop growth modeling to assess the variability of greenhouse tomato yield caused by spatial temperature variations. Comput Electron Agr 65:219–227. http://dx.doi.org/10.1016/j.compag.2008.10.001.
5. Campiotti, C., Dondi, F., Di Carlo, F., Scoccianti, M., Alonzo, G., Bibbiani, C., Incrocci, L., 2011. Preliminary results of a PV closed greenhouse system for high irradiation zones in south Italy. Acta Hort. (ISHS) 893:243–250. 10.17660/ActaHortic.2011.893.18.
6. Carlini, M., Honorati, T., Castellucci, S., 2012. Photovoltaic Greenhouses: Comparison of Optical and Thermal Behaviour for Energy Savings. Math Probl Eng Article ID 743764, 10 pages. http://dx.doi.org/10.1155/2012/743764.
7. Carlini, M., Villarini, M., Esposto, S., Bernardi, M., 2010. Performance Analysis of Greenhouses with Integrated Photovoltaic Modules, in: Taniar, D., Gervasi, O., Murgante, B., Pardede, E., Apduhan, B.O. (Eds.), Computational Science and Its Applications – ICCSA 2010, Lecture Notes in Computer Science 6017, Part II, Springer Berlin Heidelberg, pp. 206–214.
8. Castellano, S., 2014. Photovoltaic greenhouses: evaluation of shading effect and its influence on agricultural performances. J Agric Engine 45 (433):168–174. http://dx.doi.org/10.4081/jae.2014.433.
9. Castellano, S., Santamaria, P., Serio, F., 2016. Solar radiation distribution inside a

448 monospan greenhouse with the roof entirely covered by photovoltaic panels. J Agric Engine
449 47 (485), 1–6. doi:10.4081/jae.2016.485.
450 10. Challa, H., 1989. Modeling for crop growth control. Acta Hort. (ISHS) 248:209–216.
451 11. Chemisana, D., Lamnatou, C., Tripanagnostopoulos, Y., 2012. The effect of Fresnel lens -
452 solar absorber systems in greenhouses. Acta Hort. (ISHS) 952: 425–432.
453 10.17660/ActaHortic.2012.952.53.
454 12. Cockshull, K.E., Graves, C.J., Cave, C.R.J., 1992. The influence of shading on yield of
455 glasshouse tomatoes. J Hort Sci 67:11–24.
456 13. Cossu, M., Murgia, L., Caria, M., Pazzona, A., 2010. Economic feasibility study of
457 semitransparent photovoltaic technology integrated on greenhouse covering structures.
458 Proceedings of the International Conference Ragusa SHWA, Work Safety and Risk
459 Prevention in Agro-food and Forest Systems. Ragusa Ibla Campus, Italy, pp. 648–655.
460 14. Cossu, M., Murgia, L., Ledda, L., Deligios, P.A., Sirigu, A., Chessa, F., Pazzona, A., 2014.
461 Solar radiation distribution inside a greenhouse with south-oriented photovoltaic roofs and
462 effects on crop productivity. Appl. Energy 133, 89–100.
463 doi.org/10.1016/j.apenergy.2014.07.070.
464 15. Cossu, M., Yano, A., Li, Z., Onoe, M., Nakamura, H., Matsumoto, T., Nakata, J., 2016.
465 Advances on the semi-transparent modules based on micro solar cells: First integration in a
466 greenhouse system. Appl. Energy 162, 1042–1051.
467 http://dx.doi.org/10.1016/j.apenergy.2015.11.002.
468 16. Dinesh, H., Pearce, J.M., 2016. The potential of agrivoltaic systems. Renew. Sust. Energy
469 Rev. 15(9):4470–4482. http://dx.doi.org/10.1016/j.rser.2015.10.024.
470 17. Dupraz, C., Marrou, H., Talbot, G., Dufour, L., Nogier, A., Ferard, Y., 2011. Combining
471 solar photovoltaic panels and food crops for optimising land use: towards new agrivoltaic
472 schemes. Renew. Energ. 36 (10):2725–2732. http://dx.doi.org/10.1016/j.renene.2011.03.005.
473 18. El-Maghlany, W.M., Teamah, M.A., Tanaka, H., 2015. Optimum design and orientation of
474 the greenhouses for maximum capture of solar energy in North Tropical Region. Energy
475 Convers Manage 105:1096–1104. http://dx.doi.org/10.1016/j.enconman.2015.08.066.
476 19. Emmott, C.J.M., Röhr, J.A., Campoy-Quiles, M., Kirchartz, T., Urbina, A., Ekins-Daukes,
477 N.J., Nelson, J., 2015. Organic photovoltaic greenhouses: a unique application for semi-
478 transparent PV?. Energy Environ. Sci. 8, 1317-1328. DOI: 10.1039/c4ee03132f.
479 20. Fatnassi, H., Poncet, C., Bazzano, M.M., Brun, R., Bertin, N., 2015. A numerical simulation
480 of the photovoltaic greenhouse microclimate. Sol. Energy 120, 575–584.
481 doi:10.1016/j.solener.2015.07.019.

21. Kadowaki, M., Yano, A., Ishizu, F., Tanaka, T., Noda, S., 2012. Effects of greenhouse photovoltaic array shading on Welsh onion growth. Biosyst Eng 111:290–297. http://dx.doi.org/10.1016/j.biosystemseng.2011.12.006.
22. Kosugi, Y., Takanashi, S., Matsuo, N., Tanaka, K., Tanaka, H., 2006. Impact of leaf physiology on gas exchange in a Japanese evergreen broad-leaved forest. Agric. For. Meteorol. 139, 182–199. doi:10.1016/j.agrformet.2006.06.009.
23. Markvart T., 2000. Solar Electricity (2nd ed). John Wiley & Sons, Chichester, UK.
24. Marrou, H., Guilioni, L., Dufour, L., Dupraz, C., Wery, J., 2013. Microclimate under agrivoltaic systems: Is crop growth rate affected in the partial shade of solar panels?. Agr. Forest. Meteorol. 177:117–132. http://dx.doi.org/10.1016/j.agrformet.2013.04.012.
25. Marucci, A., Cappuccini, A., 2016a. Dynamic photovoltaic greenhouse: Energy efficiency in clear sky conditions. Appl. Energy 170, 362–376. doi:10.1016/j.apenergy.2016.02.138.
26. Marucci, A., Cappuccini, A., 2016b. Dynamic photovoltaic greenhouse: Energy balance in completely clear sky condition during the hot period. Energy 102, 302–312. doi:10.1016/j.energy.2016.02.053.
27. Marucci, A., Monarca, D., Cecchini, M., Colantoni, A., Manzo, A., Cappuccini, A., 2012. The semitransparent Photovoltaic Films for Mediterranean Greenhouse: A New Sustainable Technology. Math Probl Eng, Article ID 451934, 14 pages. http://dx.doi.org/10.1155/2012/451934.
28. Minuto G, Tinivella F, Bruzzone C, Minuto A. Con il fotovoltaico sul tetto la serra raddoppia la sua utilità. Supplemento a L'Informatore Agrario 2011; 38:2–6.
29. Minuto, G., Bruzzone, C., Tinivella, F., Delfino, G., Minuto, A., 2009. Fotovoltaico sui tetti delle serre per produrre anche energia. Supplemento a L'Informatore Agrario 2009; 10:16–21.
30. Page, J., 2003. The role of solar radiation climatology in the design of photovoltaic systems. In: Practical Handbook of Photovoltaics: Fundamentals and Applications (Markvart T; Castañer L eds), pp. 5–66. Elsevier, Oxford, UK.
31. Palva, L., Markkanen, T., Siivola, E., Garam, E., Linnavuo, M., Nevas, S., Manoochehri, F., Palmroth, S., Rajala, K., Ruotoistenmäki, H., Vuorivirta, T., Seppälä, I., Vesala, T., Hari, P., Sepponen, R., 2001. Tree scale distributed multipoint measuring system of photosynthetically active radiation. Agric. For. Meteorol. 106, 71–80. doi:10.1016/S0168-1923(00)00171-4.
32. Poncet, C., Muller, M.M., Brun, R., Fatnassi, H., 2012. Photovoltaic greenhouses, non-sense or a real opportunity for the greenhouse systems?. Acta Hort. (ISHS) 927, 75–79. 10.17660/ActaHortic.2012.927.7.

517 33. Reiter, R., Munzert, K., Sladkovic, R., 1982. Results of 5-year concurrent recordings of
518 global, diffuse, and UV-radiation at three levels (700, 1800, and 3000 m a.s.l.) in the
519 northern Alps. Theor. Appl. Climatol. Series B 30, 1–28.
520 34. Serrano-Arellano, J., Gijón-Rivera, M., Chávez-Servín, J.L., de la Torre-Carbot, K., Xamán,
521 J., Álvarez, G., Belman-Flores, J.M., 2015. Numerical study of thermal environment of a
522 greenhouse dedicated to amaranth seed cultivation. Sol. Energy 120:536–548.
523 http://dx.doi.org/10.1016/j.solener.2015.08.004.
524 35. Sethi, V.P., 2009. On the selection of shape and orientation of a greenhouse: Thermal
525 modeling and experimental validation. Sol. Energy 83:21–38.
526 http://dx.doi.org/10.1016/j.solener.2008.05.018.
527 36. Sethi, V.P., Dubey, R.K., 2011. Development of dual purpose greenhouse coupled with
528 north wall utilization for higher economic gains. Sol. Energy 85:734–745.
529 http://dx.doi.org/10.1016/j.solener.2011.01.004.
530 37. Sonneveld, P.J., Swinkels, G.L.A.M., Tuijl, B.A.J. van, Janssen, H.J.J., Campen, J., Bot,
531 G.P.A., 2011. Performance of a concentrated photovoltaic energy system with static linear
532 Fresnel lenses. Sol. Energy 85:432–442. doi:10.1016/j.solener.2010.12.001.
533 38. Tanaka, K., Kosugi, Y., Nakamura, A., 2002. Impact of leaf physiological characteristics on
534 seasonal variation in CO2, latent and sensible heat exchanges over a tree plantation. Agric.
535 For. Meteorol. 114, 103–122. doi:10.1016/S0168-1923(02)00128-4.
536 39. Ureña-Sánchez, R., Callejón-Ferre, Á.J., Pérez-Alonso, J., Carreño-Ortega, Á., 2012.
537 Greenhouse tomato production with electricity generation by roof-mounted flexible solar
538 panels. Sci Agr 69 (4):233–239. http://dx.doi.org/10.1590/S0103-90162012000400001.
539 40. Wolfram Research, Inc., Mathematica, Version 10.0, Champaign, IL (2014).
540 41. Yano, A., Furue, A., Kadowaki, M., Tanaka, T., Hiraki, E., Miyamoto, M., Ishizu, F., Noda,
541 S., 2009. Electrical energy generated by photovoltaic modules mounted inside the roof of a
542 north-south oriented greenhouse. Biosyst. Eng. 103 (2):228–238.
543 http://dx.doi.org/10.1016/j.biosystemseng.2009.02.020.
544 42. Yano, A., Kadowaki, M., Furue, A., Tamaki, N., Tanaka, T., Hiraki, E., Kato, Y., Ishizu, F.,
545 Noda, S., 2010. Shading and electrical features of a photovoltaic array mounted inside the
546 roof of an east-west oriented greenhouse. Biosyst Eng 106:367–377.
547 http://dx.doi.org/10.1016/j.biosystemseng.2010.04.007.
548 43. Yano, A., Onoe, M., Nakata, J., 2014. Prototype semi-transparent photovoltaic modules for
549 greenhouse roof applications. Biosyst Eng 122:62–73.
550 http://dx.doi.org/10.1016/j.biosystemseng.2014.04.003.
551

552 **FIGURE CAPTIONS**

553 **Fig. 1.** Map of the PV greenhouse and position of the sets of OPs for the calculations. The OPs in
554 grey and alphabet letters indicate the position of the pyranometers used for validating the model.
555 The x and y axis for the Cartesian coordinates of the PV panels and the OPs are also displayed.

556 **Fig. 2.** Solar elevation angle and azimuth angle of the sun, in relation to the position of the PV panel
557 and the observation point OP. The case 1 depicts a position of the sun in which the OP is under
558 direct sunlight; in case 2 the OP is under the shading of the PV panel. θ and Ψ are the solar
559 elevation and the solar azimuth angles, respectively.

560 **Fig. 3.** Flow chart of the calculation and decisional process operated by the model via software.

561 **Fig. 4.** Solar coordinates of the PV array and the sun path on the OP F at 1.3 m height (a), and
562 related global radiation (b) during three exemplifying days with no shading (June 16, 2013 τ=0.70,
563 R^2=0.97), partial shading (September 14, 2013, τ=0.60, R^2=0.84), and complete shading (December
564 14, 2013, τ=0.49, R^2=0.97). All days were with clear sky conditions during measurements. In figure
565 4b: dashed curve is the measured I_G, grey line is the measured I_{GP} and black line is the calculated
566 I_{GP}.

567 **Fig. 5.** Cumulated monthly distribution expressed as G_{GR} (%) on the greenhouse transversal
568 direction (N-S) on 1.0 m height and estimated shadow path; p=0.65, τ=0.60.

569 **Fig. 6.** Maps of the cumulated yearly light distribution on the PV greenhouse area, expressed as
570 G_{GR} (%) at different canopy heights: ground level, 0.5 and 1.5 m; p=0.65, τ=0.60.

571 **Tab. 1.** Monthly cumulated global radiation at different canopy heights under the plastic cover, the
572 PV cover and on the whole greenhouse area. Data are expressed as G_{GR} (%). p=0.65, τ=0.60.

Tab. 1. Monthly cumulated global radiation at different canopy heights under the plastic cover, the PV cover and on the whole greenhouse area. Data are expressed as G_{GR} (%). p=0.65, τ=0.60.

Months	***0.0 m***			***0.5 m***			***1.0 m***			***1.5 m***			***2.0 m***		
	Plastic	***PV***	***Greenhouse***	***Plastic***	***PV***	***Greenhouse***	***Plastic***	***PV***	***Greenhouse***	***Plastic***	***PV***	***Greenhouse***	***Plastic***	***PV***	***Greenhouse***
January	38	77	56	37	74	53	37	66	50	36	58	46	41	44	44
February	33	77	53	33	70	50	36	60	48	44	48	47	55	32	45
March	43	61	52	50	55	53	57	45	51	65	38	52	72	28	50
April	71	45	58	75	40	57	80	34	57	84	29	56	88	34	60
May	88	36	61	90	31	60	92	31	61	95	35	63	98	45	70
June	92	31	61	93	32	62	97	34	65	100	41	69	100	54	75
July	90	33	61	92	31	61	93	33	62	97	38	66	100	49	73
August	78	40	58	82	36	58	85	30	57	89	30	59	92	38	63
September	55	57	56	61	49	55	67	42	55	73	33	53	80	30	55
October	35	74	54	38	66	52	44	57	51	53	44	49	61	30	46
November	40	79	58	39	75	55	38	67	51	40	57	48	46	42	45
December	45	75	61	42	74	57	41	69	54	41	59	49	41	48	45
Yearly mean	**59**	**57**	**57**	**61**	**53**	**56**	**64**	**47**	**55**	**68**	**42**	**55**	**73**	**40**	**56**

Figure 1. PV Greenhouse Map

Click here to download high resolution image

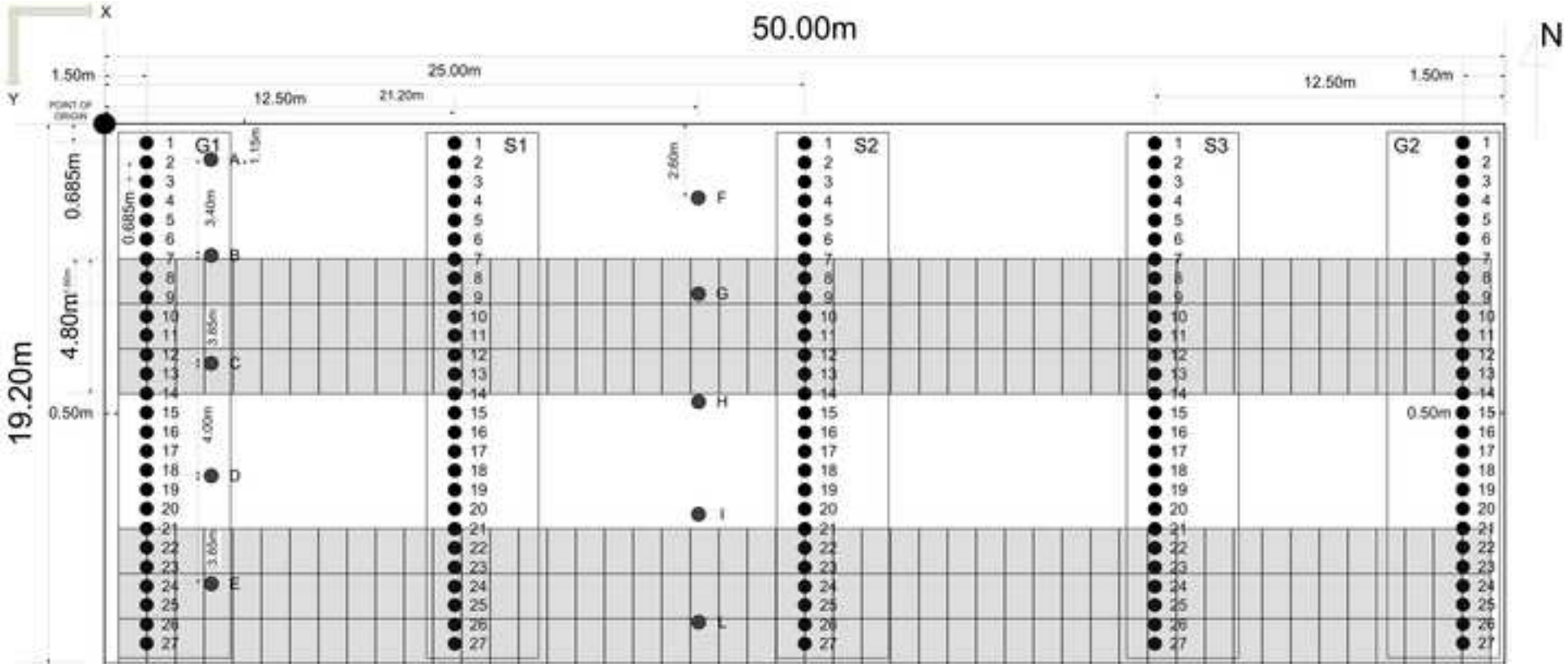

Figure 2. Solar Coordinates

Click here to download high resolution image

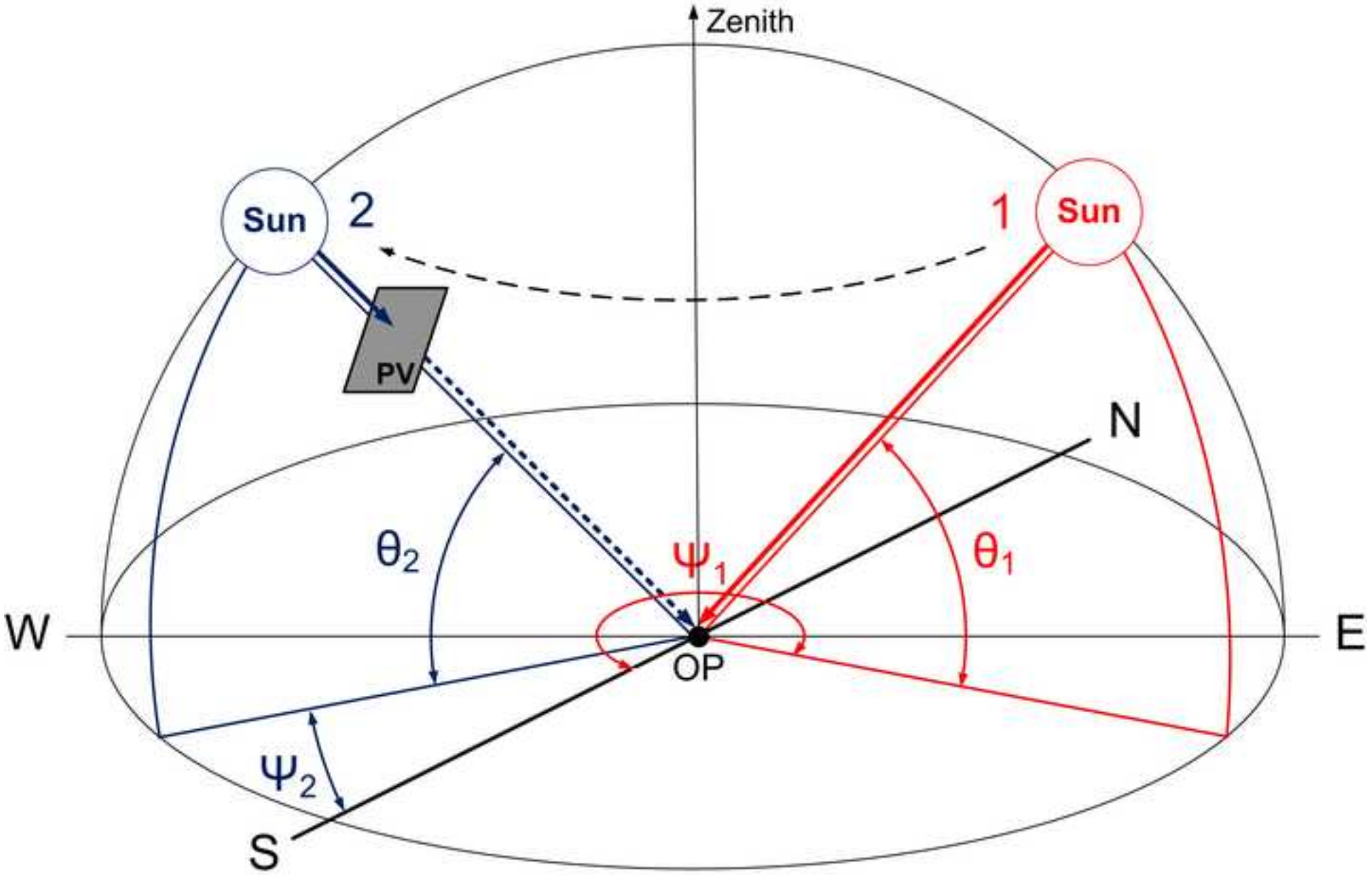

Figure 3. Algorithm flow chart

Click here to download high resolution image

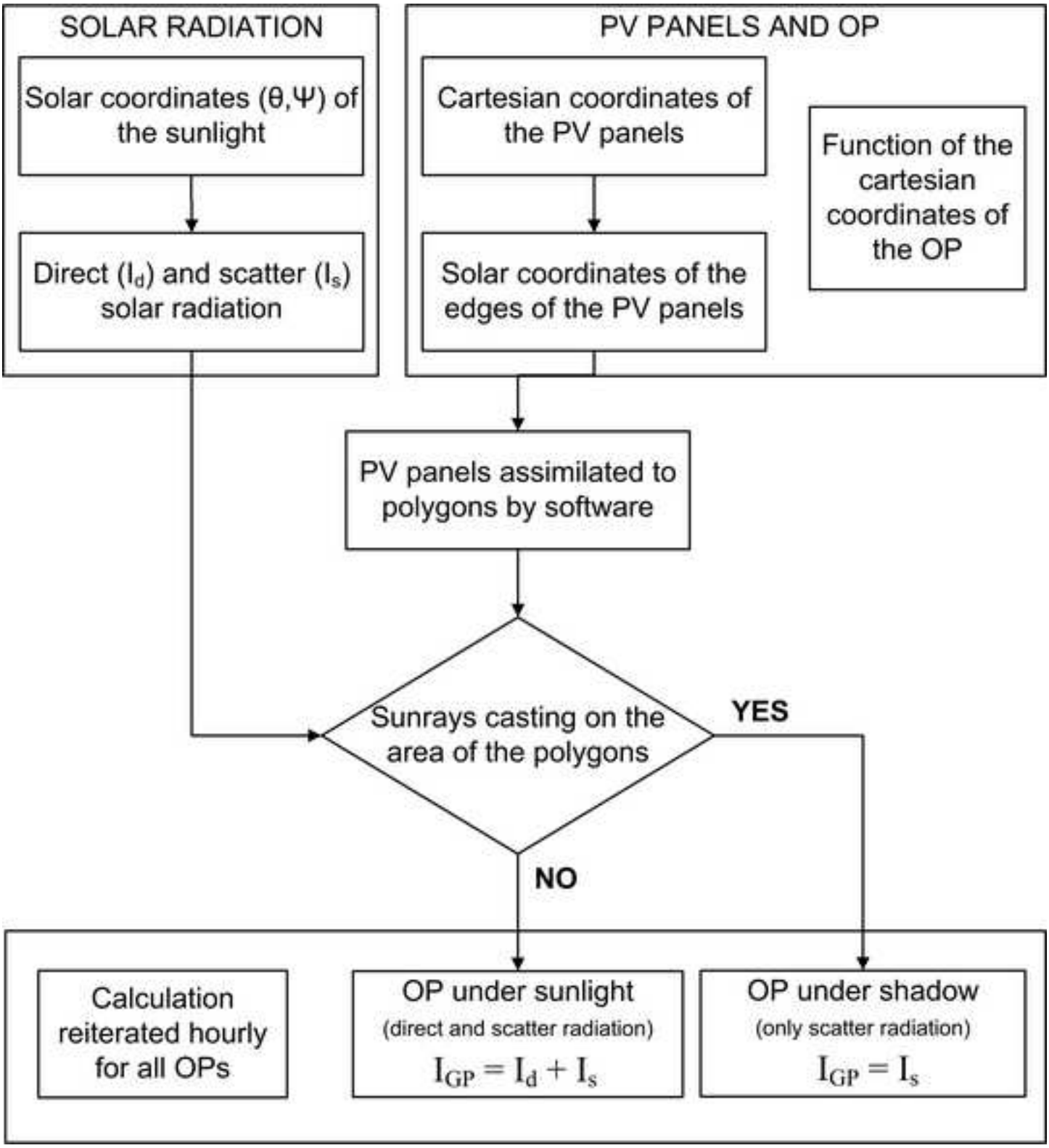

Figure 4. Solar coordinates and global radiation
Click here to download high resolution image

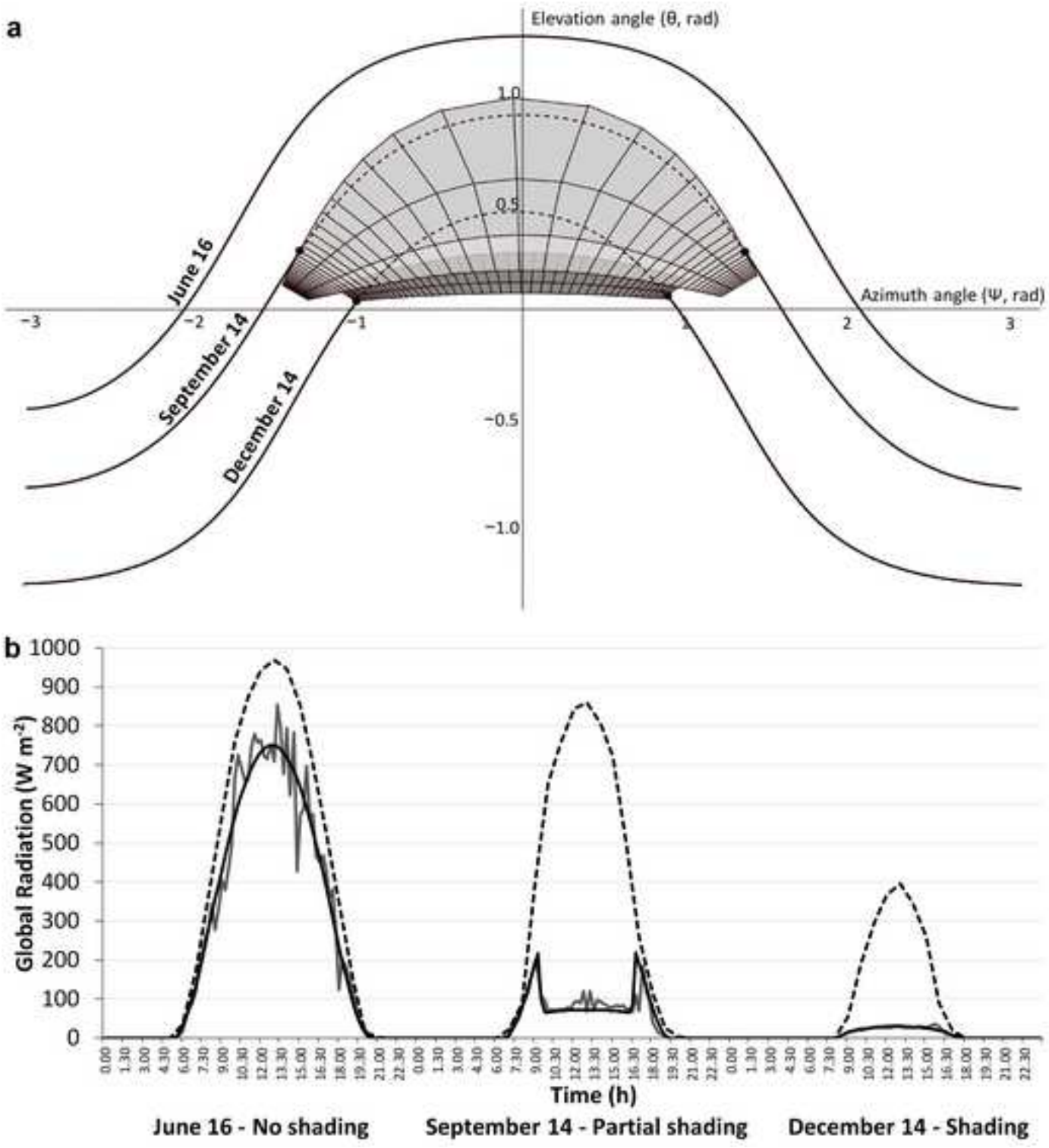

Figure 5. Monthly distribution

Click here to download high resolution image

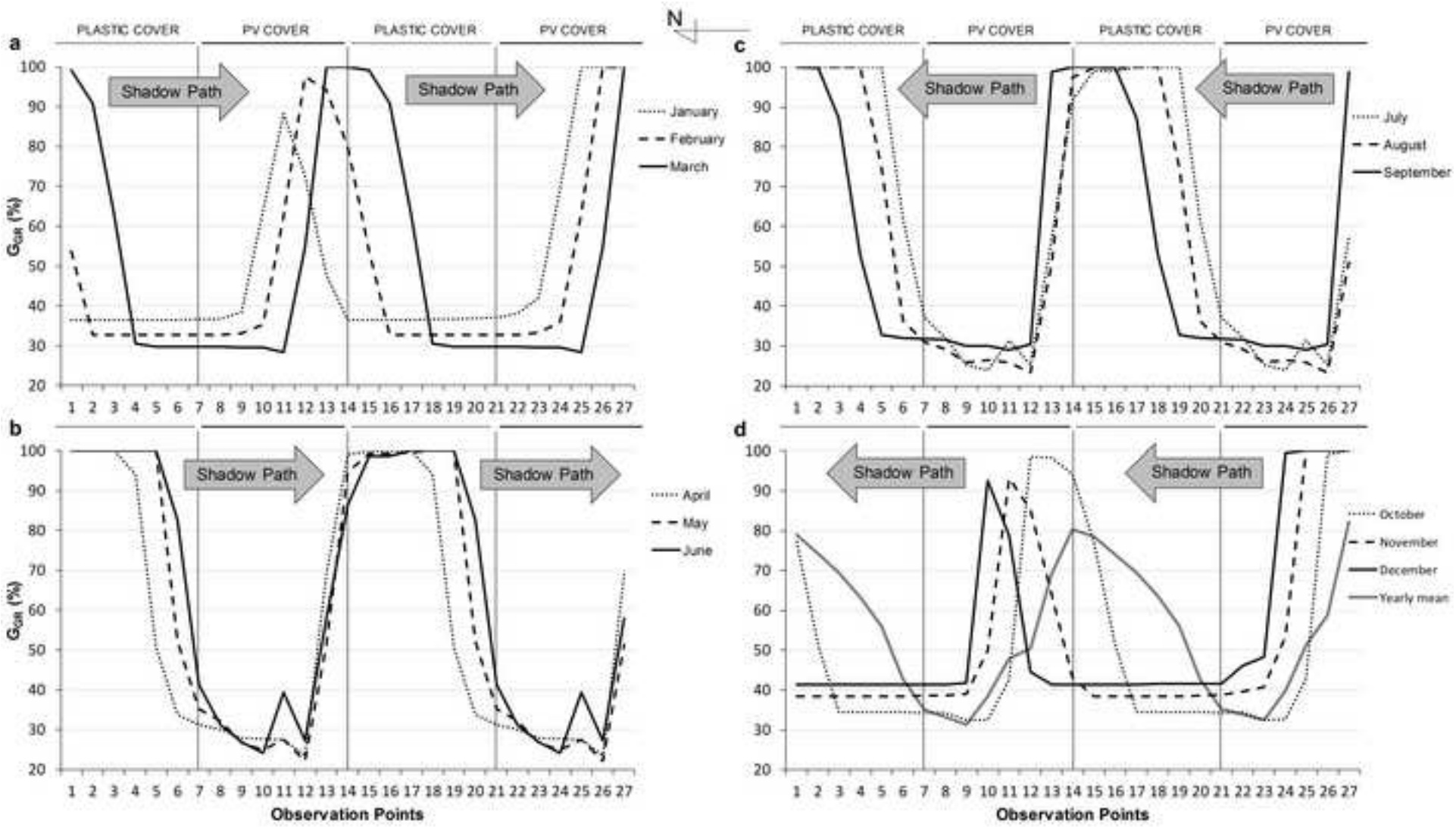

Figure 6. Yearly light distribution maps

Click here to download high resolution image

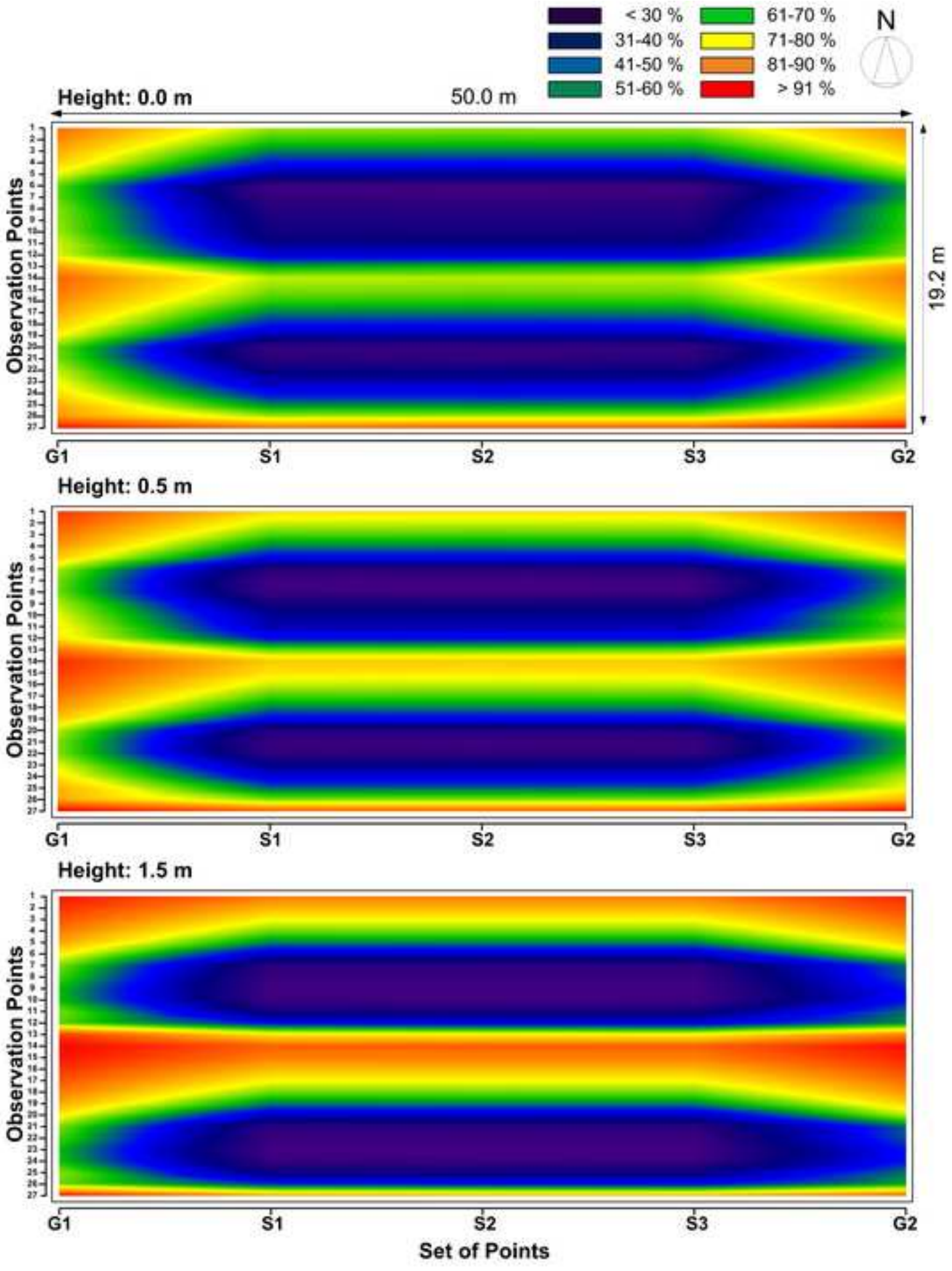

HIGHLIGHTS

- The cumulated global radiation inside photovoltaic (PV) greenhouses was calculated.
- An algorithm for the calculation at the desired time interval was elaborated.
- Results were used to draw maps of light distribution on different canopy heights.
- The light distribution changed consistently, according to the height of the canopy.
- The algorithm can be applied to different PV greenhouse types.